

Geometric constraints on the dynamics of networks

Gabriel A. Silva*

Department of Bioengineering
University of California, San Diego

Abstract

In any physically constructible network there is a structure-function relationship between the geometry of the network and its dynamics. The network's geometry, i.e. its physical structure, constrains and bounds signaling and the flow of information through the network. In this paper we explore how the physical geometry of a network constrains and ultimately determines its dynamics. We construct a formal theoretical framework of the relationship between network structure and function and how information flows through a network. One interesting result of this work is that we show how a strictly local process at the scale of individual node pairs directly affects the behavior of the system at the whole network scale. Individual nodes responding to information from the upstream nodes it is connected to produce the observable emergent dynamics of the entire network at a global scale, independent of and without any knowledge of what all the other nodes in the network may be doing. This analysis does not rely on statistical metrics that characterize a network at the whole network scale, but rather, makes use of the nature by which the structure and geometry of physically constructible networks necessarily constrain information flow given the internal state dynamics of individual nodes. This is a fundamental yet intuitive result. This approach can also be used for the systematic *design* of networks that need to meet specific design criteria and behaviors. We then provide empirical evidence that at least some important examples of both naturally occurring and engineered networks are capable of approaching a state of optimal dynamical efficiency, one of the key results of the theory. While we progressively build up to what this formally means, informally it means that these networks have evolved or have been designed to optimize how they are able to handle the processing of information by matching the dynamical requirements of individual nodes to the flow of information (i.e. signals) between nodes in the network. In different ways, we use the theory to investigate properties of pyramidal neurons in biological neural networks in the visual cortex, the prevalence of the small world network topology, and the internet router network.

*Corresponding author: Prof. Gabriel A. Silva
UC San Diego Jacobs Retina Center
9415 Campus Point Drive
La Jolla, California 92037-0946

Email: gsilva@ucsd.edu
Tel. 858.822.4591

1 Introduction

In any physically constructible network there is a structure-function relationship between the geometry of the network and its dynamics. The network's geometry, i.e. its physical structure, constrains and bounds signaling and the flow of information through the network. Historically however, the modeling and analysis of complex networks has focused either on the temporal evolution and transition of the states of the nodes, or the network connectivity topology and its effects on statistical metrics that characterize the network as a whole. The former is an extension of classical dynamical systems theory, while the latter is derived from statistical mechanics [18]. More recently, researchers have begun to consider the co-evolution of node states in conjunction with the evolution of a network's connectivity topology, referred to as adaptive networks. While this approach is still at a very early stage both conceptually and mathematically, the relevance of adaptive networks as models of real world networks is intuitively appealing. In any physically constructible network there must exist a reciprocal relationship between the internal dynamical states of its nodes and how those nodes communicate with each other, i.e. its connectivity, that is ultimately determinant of the global properties of the network. In other words, what the network can do. Understanding such dynamics is now recognized as one of the most important open problems in the study of complex networks [1, 8, 10, 11, 18].

In this paper we explore how the physical geometry of a network constrains and ultimately determines its dynamics. We construct a formal theoretical framework of the relationship between network structure and function and how information flows through a network. One important result of this work is that we show how a strictly local process at the scale of individual node pairs directly affects the behavior of the system at the whole network scale. Individual nodes responding to information from the upstream nodes it is connected to produce the observable emergent dynamics of the entire network at a global scale, independent of and without any knowledge of what all the other nodes in the network may be doing. This analysis does not rely on statistical metrics that characterize a network at the whole network scale, but rather, makes use of the nature by which the structure and geometry of physically constructible networks necessarily constrain information flow given the internal state dynamics of individual nodes. This is a fundamental yet intuitive result. This approach can also be used for the systematic *design* of networks that need to meet specific design criteria and behaviors.

Another key result is a theoretical definition of optimal dynamical efficiency of a network. While we progressively build up to what this formally means, informally it means that these networks have evolved or have been designed to optimize how they are able to handle the processing of information by matching the dynamical requirements of individual nodes to the flow of information (i.e. signals) between nodes in the network. It is a form of self-organized criticality. This result directly falls out of the theory and suggests how working in reverse, starting with the theory and working towards the design of a network, an optimally efficient network can be constructed. We then provide empirical evidence that at least some important examples of both naturally occurring and engineered networks are capable of approaching such a state of optimal dynamical efficiency. In different ways, we use the theory to investigate properties of pyramidal neurons in biological neural networks in the visual cortex, the prevalence of the small world network topology, and the internet router network.

The paper is organized as follows: Section 2 presents an intuitive motivating example for this work drawn from our own past work in systems neuroscience. In section 3.1 we enumerate a number of technical definitions and preliminary concepts that we use for the development of the theory and throughout other sections of the paper. Section 3.2 introduces the model (competitive refractory dynamics) which underlies the analysis of the network’s dynamics. Section 3.3 and its sub-sections then provide a detailed analysis of the dynamics. In section 4.1 we present the major theoretical result, and derive upper and lower bounds for optimal dynamical efficiency within the context of the developed theory. The next section 5 and its sub-sections discuss optimized efficiency in the three examples and provide varying interpretations of the theory for each. Finally, section 6 is a brief concluding and discussion section that outlines possible applications of the theory, directions for future research, and possible theoretical links to other work.

2 A motivating example: Geometric neuronal network dynamics

Conceptually, the framework we develop describes a relationship between the dynamics of signal flows along the edges of a network relative to how quickly the internal ‘machinery’ of a node is able to process and react to an incoming signal. In this paper we show how optimal dynamical efficiency is achieved by a balance between how fast information is capable of propagating through the network relative to how quickly its nodes can process incoming signals. Too much too fast is not necessarily always best. We prove that the internal dynamical processing of signals by individual participating nodes, i.e. how long it takes the internal machinery of the node to act’ on an incoming signal, must be temporally matched to the speed at which signals are propagating between nodes in the first place. If this is too fast or too slow it results in sub-optimal network dynamics. As an example, we have previously shown numerically in a simulated neuronal network consisting of Izhekivitch neurons (a model of the internal neuronal machinery responsible for the generation of action potentials in each neuron) that the ability of the network to sustain recurrent signaling is a function of this balance [6] (Fig. 1). Computationally such a network can be reduced to a relationship between the positions of the neurons in space (or in the plane) and the temporal delays with which signals propagate between them. The longer, e.g. more convoluted, a process is the longer it will take a signal to reach from one neuron to another. In recurrent distributed networks like biological neural networks the relationship between network geometry and signaling delays serves as a form of signal storage, essentially giving the neurons time to recover from the refractory period between activations, which in turn results in information rich sustainable recurrent signaling, but only if the internal dynamics match the network signaling dynamics. In Fig. 1, the network shown in panels a. and b. was driven by an external input for the first 500 ms. If the signaling speeds were too fast (200 pixels/ms in the example here) incoming signals from upstream neurons never had an opportunity to activate downstream cells because they were still refractory and not able to respond. This led to unsustainable signaling that quickly died away (Fig. 1c. bottom panel). As the signaling delays increased at an appropriate rate, recurrent sustained activity emerged (at a signaling speed of 20 pixels/ms: panel c., middle), and became stable as the signaling speed matched the neuronal dynamics (2 pixels/ms, panel c, top). Note that no parameter other than the signaling speed (or inversely, signaling delays) on the edges connecting the nodes changed between

the three numerical experiments in panel c. The geometric structure of the network, including its physical connectivity, the internal model of the dynamics of individual neurons, and the coupling (synaptic) weights between connected neurons did not change. Only the signaling speed. This description provides an intuitive and simple explanation of the observed data and the behavior of the network. However, there is *no* analytic theoretical framework capable of describing or predicting such dynamics, or capable of computing or analyzing the boundary conditions of different dynamic behaviors. As a result, we wanted to develop an appropriate mathematical framework that could achieve this, and provide both descriptive and predictive insights into such network dynamics.

3 Theoretical development

We begin by describing a dynamic model that computes how a given node responds to and processes incoming signals from different upstream nodes that connect to it. The foundational premiss is that if a node is in an internal state in which it is capable of responding to upstream nodes, the signal that reaches it first will 'win' and the node will process that signal in order to make a decision about whether to output a signal in turn. As the node internally processes such a signal it necessarily remains refractory, i.e. displays a refractory period, to other incoming signals. The details of how one defines such a refractory period will vary depending on the physical details of the system under consideration, but it effectively represents any finite amount of time it takes a node to react to, process, or otherwise manipulate an incoming signal in a meaningful way that results in some form of output. Following this refractory period it will once again be in a state in which it can accept or respond to another input. A few key considerations determine what upstream node is the winning node at any instantaneous moment in time. These include the path length (distance) in the connection to the target node, the signaling speed, or its inverse, the temporal signaling delay between two connected nodes, and the refractory period of a the target node, which is determined by its internal dynamic model. Clearly the path lengths between nodes is a function of the network's physical connectivity. In the trivial case where a node is not refractory and all its connected upstream nodes signal the target node at the exact same moment at the exact same signaling speed computing the winning node is simply determined by the shortest path length, i.e. the shortest connection. However, the situation becomes more interesting when one considers not just different path lengths, but simultaneously temporal offsets in when different upstream nodes initiate a signal and differing amounts of temporal progression in the recovery of the refractory period of the target node at the moment the network is observed, its effective refractory period. The theoretical analysis that follows arrives at a condition that allows computing which signal from incoming nodes wins at any given instantaneous moment given all these interactions.

3.1 Definitions and preliminaries

We define a network as a physically realizable and constructible structure consisting of nodes with unique internal dynamics and a physical connectivity in space between specific pairs of nodes. Because it is a physical network there must exist a finite signaling speed for the propagation of information between nodes and a finite temporal delay associated with the flow of information

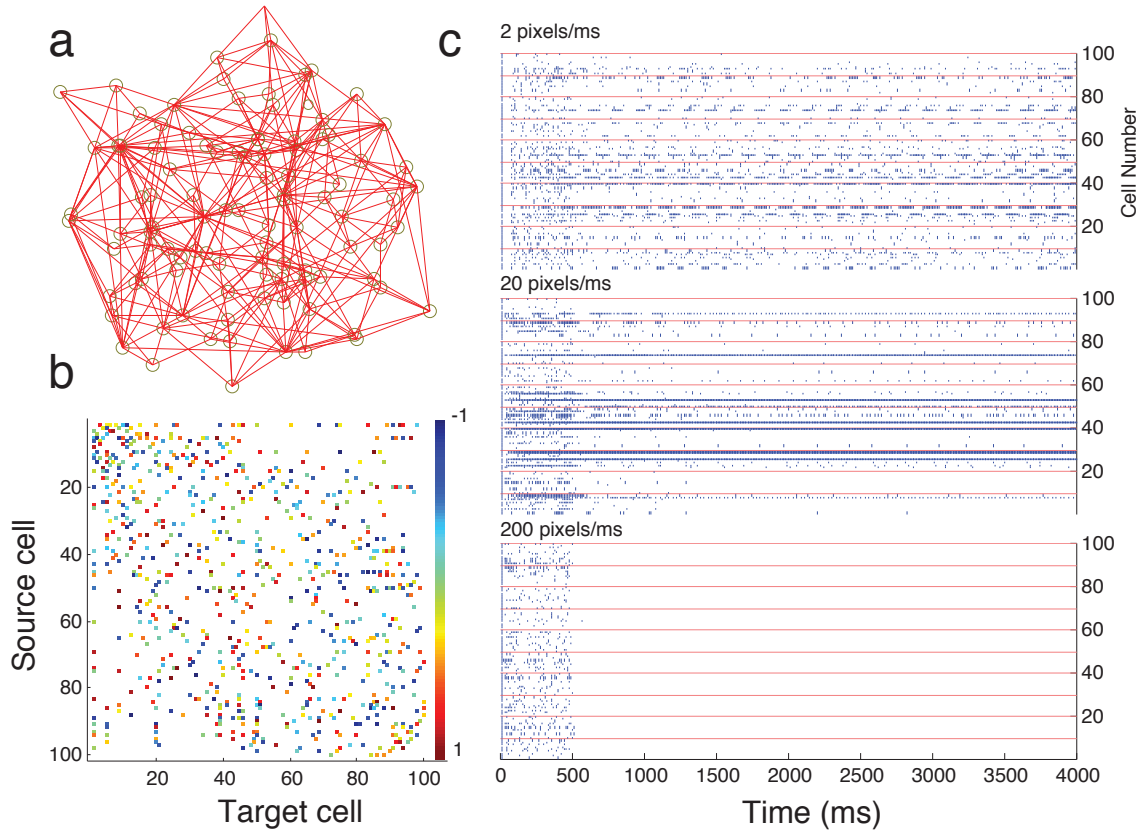


Figure 1: Relationship between network geometry, signaling delays and their effect on network dynamics. The three dimensional geometric network shown in panel A was assigned random weights uniformly distributed between -1 and 1 on each physical edge (panel B). An Izhikevitch model of bursting neurons was used to model the individual vertex dynamics. C. By varying the speed of signal propagations between cells (in arbitrary units of pixels/ms), signaling delays have a critical impact on the resultant spike dynamics. See text for details. Adapted from [6].

between nodes. Formally, we will consider graph models of such physical networks. In general we will explicitly refer to the graph model of a network, and therefore refer to the vertices and edges of the graphs, but it should be understood that they model the nodes and connections of the physical network of interest. At times we will interchange the terminology between vertices and nodes, and connections and edges, when there is no chance for confusion.

We consider the flow of information, or signaling, along the path lengths of directed edges that have a physical representation in space (or the plane) that connect two vertices of the graph in space (or the plane; fig. 2). In this sense edges are represented by smooth and continuous Jordan arcs. Such a graph represents a model of a physically constructible network, in that any real world network can be modeled as such a graph. The term 'geometric graph' is often used in a somewhat ambiguous way depending on the author or context. Topological graph theory typically refers to the embedding and study of graphs in some topological space, including three dimensional Euclidean spaces and surfaces [2,3]. However, other authors for example have distinguished geometric graphs from topological graphs as graphs in the plane with distinct points connected by straight line edges in the former case versus graphs in the plane with distinct points connected by Jordan arcs in the latter case, i.e. both in \mathbb{R}^2 [15]. In this paper we only need to consider graphs with a physical representation in the Euclidean plane \mathbb{R}^2 or three dimensional space \mathbb{R}^3 , and not in any other topological space. As such, we will use the term 'geometric graph' to refer to any graph in \mathbb{R}^2 or \mathbb{R}^3 . We formalize these notions below.

Definition 3.1. *A graph is an ordered pair of finite disjoint sets $G = (v, E)$ such that v is the set of vertices in the graph and E is the set of edges joining the vertices.*

Definition 3.2. *A geometric graph $G = (\bar{v}, E)$ is a graph who's vertices have a physical position in \mathbb{R}^2 or \mathbb{R}^3 in some appropriate coordinate system. Physical coordinates $\bar{v}_i := \bar{x}$ for an ordered triplet $\bar{x} = (x_1, x_2, x_3)$ are assigned to each vertex v_i for all vertices $i = 1 \dots N$ in the graph, with the set of all vertices given by $\bar{v} = \{v_i\}$ [6].*

Definition 3.3. *A complete geometric graph $G = (\bar{v}, \bar{E})$ is a geometric graph with directed edges that also have a physical definition in space: An edge e_{ij} is defined if there is a directed connection from vertex i to vertex j . Let an edge between vertices i and j be defined geometrically as $e_{ij} = f(\bar{x})$ for some function $f(\cdot)$ in \mathbb{R}^3 , restricted to simple non-intersecting Jordan arcs. The physical distance of the edge between any two vertices is determined by the path integral taken by the edge in space where for some scalar field $f : U \subseteq \mathbb{R}^n \rightarrow \mathbb{R}$. The path integral d_{ij} from \bar{v}_i to \bar{v}_j formed by a piecewise smooth curve $C \subset U$ is defined as*

$$|e_{ij}| = d_{ij} := \int_C f ds = \int_{\bar{v}_i}^{\bar{v}_j} f(\bar{r}(t)) |\bar{r}'(t)| dt$$

where $r : [\bar{v}_i, \bar{v}_j] \rightarrow C$ is an arbitrary bijective parametrization of the curve C such that $r(\bar{v}_i)$ and $r(\bar{v}_j)$ give the endpoints of C for $\bar{v}_i < \bar{v}_j$.

As a technical comment, it should be noted that our use of the term 'complete geometric graph' here differs from the use of the term 'complete graph' referring to a simple undirected graph in which every pair of distinct vertices is connected by a unique edge, or that of a complete digraph which is a directed graph in which every pair of distinct vertices is connected by a pair of unique edges.

In addition, we do not notationally distinguish between 'geometric graph' and 'complete geometric graph', i.e. between definitions 3.2 and 3.3 in the rest of this paper in order to avoid introducing additional (unnecessary) notation. This distinction is not necessary because we strictly deal with complete geometric graphs in the work that follows, and the notation $G = (\bar{v}, \bar{E})$ should be assumed to refer accordingly.

Definition 3.4. *The set of all geometric edges for the geometric graph $G = (\bar{v}, \bar{E})$ is given by $\bar{E} = \{e_{ij}\}$ for all existing edges.*

Definition 3.5. *We distinguish a non-minimal complete geometric graph, denoted by G , from the 'minimal' complete geometric graph representation G_{min} , in the sense that the edges of G_{min} are all (geodesic) straight line edges, i.e. \bar{E}_{min} with $\langle d_{ij} \rangle_{min} < d_{ij}$, for any edges d_{ij} in \mathcal{G} .*

The graphs G_{min} and G share the same vertex set \bar{v} and structural (physical) connectivity, but the edge set of G_{min} given by \bar{E}_{min} are straight lines while the edge set of G given by \bar{E} follow longer convoluted geometric paths in space determined by the actual physical nature of the network under consideration, *c.f.* definition 3.3 above. As an example of this distinction, consider the network shown in fig. 2. From a classical graph theoretic perspective both networks in panels a. and b. are equivalent because they have the same connectivity and adjacency matrix. However, dynamically, the delay associated with the arrival of a signal propagating along an edge at a constant finite speed will be a function of the propagation speed and path length of the edge. This consideration is critical for computing the dynamics of the network as a whole for nodes that require a finite amount of processing time associated with how they use and respond to any incoming signals. Real world networks typically look much more like the network in panel b. than the one in a., such as for example the two brain network reconstructions in panels c. and d. (see figure legend for details). Mathematically though, there will exist a mapping from $G \rightarrow G_{min}$ by increasing or decreasing the temporal delays in G_{min} to match those that would occur in G . However, this is not always possible and it is not always obvious how to produce such a mapping when considering real world networks, and it often leads to an over simplification and loss of insights into the physical mechanisms that underlie the dynamics and behavior of the network. And while we will not explicitly use this definition in this paper, we introduce it for completeness. This definition will play a much more central role in a sequel to this paper.

Definition 3.6. *The subgraph H_j is the reverse geometric tree that consists of all vertices v_i with directed geometric edges into v_j . We write $H_j(v_i)$ to represent the set of all vertices v_i in H_j and $H_j[v_i]$ to refer to a specific $v_i \in H_j(v_i)$.*

Definition 3.7. *The edge set of H_j is denoted by $H_j(E)$*

Definition 3.8. *There exists a signaling speed s_{ij} for the flow of a signal (information) on the edge e_{ij} .*

Corollary 3.9. *$0 < s_{ij} < \infty$ for any physically realizable network, i.e. it must be finite.*

Definition 3.10. *The absolute refractory period of a vertex v_j is given by R_j , determined by a given internal dynamic model of the node being represented by the vertex v_j .*

What constitutes R_j and the processes that contribute to it will depend on the physical details of individual networks, but it represents the summation of any and all dynamical processes in v_j that

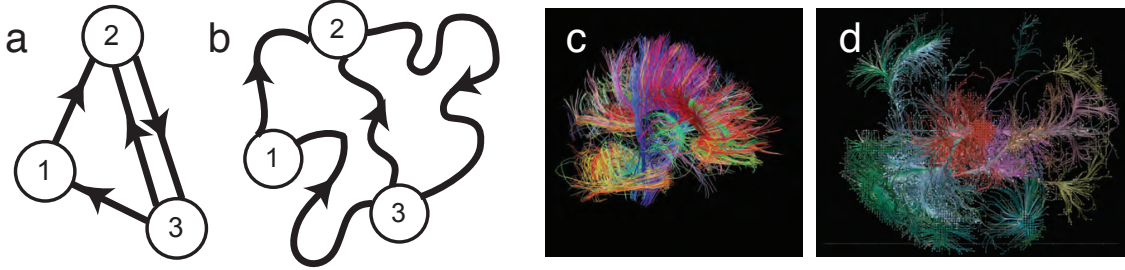


Figure 2: Classical versus complete geometric graph models of networks. Complete geometric graphs as we define them here are defined as graphs whose vertices have a physical position in space (or the plane), with directed edges that also have a physical (path integral) representation in space (or the plane). **a.** A classical representation of a graph consisting of vertices connected by edges, where the only important consideration is the connectivity of the vertices (i.e. adjacency matrix). There is no geometric significance to how the graph is drawn. **b.** A ‘non-minimal’ complete geometric representation of the same graph (see text for definitions and details of our use of this terminology). While both networks in panels a. and b. are equivalent in classical graph theory, they are very different as we define them here, with their structures directly determining their dynamics. **c and d.** Experimental reconstructions of brain networks. Panel c. shows a diffusion spectral imaging (DSI) MRI reconstruction of white matter tracts in the human brain, while panel d. shows a partial cellular connectome fluorescent protein viral reconstruction of between 100 to 500 neurons in the mouse brain. Qualitatively, these examples of real world complex networks resemble the complete geometric graph in panel b much more than the classical rendering of a graph in panel a. (Panel c. data adapted from The Human Connectome Project (www.humanconnectomeproject.org). Panel d. adapted from Oh et. al (2014) Nature 508:207.)

contribute to a processing delay from the instant a signal arrives at v_j to the moment when the node produces some actionable output as a causal response to the input.

Corollary 3.11. $R_j > 0$ for any physically realizable network, i.e. there cannot exist an infinitely fast or instantaneous response. See Section 3.2.

Definition 3.12. By $H_j[v_i] \rightsquigarrow v_j$ we mean a vertex $v_i \in H_j$ that causally leads to the activation of v_j .

3.2 Competitive refractory dynamics

Consider a vertex v_i with a directed geometric edge to a vertex v_j . The length of the edge can be the minimum geodesic, a straight line $\langle d_{ij} \rangle_{min}$ in \mathbb{R}^3 , or it can be a spatially convoluted path such that $d_{ij} > \langle d_{ij} \rangle_{min}$, c.f. definition 3.3. For v_i to signal or communicate with v_j , there must be some physical signal s_{ij} representing a flow of information from v_i to v_j over the edge that connects them which travels at some finite speed (c.f. corollary 3.9). Note that in the following development we assume that s_{ij} is a constant value s for all edges in the network, but this need not be in the general

case. We briefly consider this in section 6 below. If v_i and v_j share the same internal dynamics, i.e. are both the same type of node and their internal dynamics can be modeled in the same way, then $R_i = R_j \equiv R$. This would be the case for example, if one were considering a homogeneous population of neurons in a specific neural circuit. In the construction of this framework, once v_j receives a signal from v_i it becomes refractory for the period R_j as determined by the internal dynamic model of the node and will not be able to respond to another incoming signal during this period of time. Note that there is no restriction on the internal dynamic model that a node can take. Again using biological neurons as an example, any model that produces an action potential could be applied (see [6] for details).

Let τ_{ij} represent the time delay it takes a signal to reach v_j from v_i . Then

$$\tau_{ij} = \frac{d_{ij}}{s} \tag{1a}$$

$$\langle \tau_{ij} \rangle_{min} = \frac{\langle d_{ij} \rangle_{min}}{s} \tag{1b}$$

which ensures that $\langle \tau_{ij} \rangle_{min} < \tau_{ij}$ always.

Let $y_j(\Omega, t)$ represent the instantaneous state of vertex j as a function of time and some parameter set Ω determined by the internal model that represents the dynamics of the node. In the context of biological neural networks we have previously defined a geometric (although not complete geometric) state space framework of network dynamics with this form and showed how such a framework can be used to represent, compute, and simulate the temporal signaling evolution of a dynamic network [6]. That previous work provided an analytical description and algorithm for computing the instantaneous internal states of a node in a geometric network and its subsequent advancement in discrete time steps using a transfer function definition of the internal model. The framework was designed to accommodate essentially any specific model of single node dynamics, and naturally extends to any physical network (not just neurobiological). For our purposes here though, how $y_j(\Omega, t)$ is computed is not of immediate concern, only that it can be. The important consideration is that the internal state can be interpreted as a binary function at any time t determined by the internal machinery of v_j that results in $y_j(\Omega, t)$. We can then define this function at a time T_o as

$$y_j(\Omega, T_o) = \begin{cases} 1, & \text{iff } v_j \text{ can respond to an input} \\ 0, & \text{iff it is refractory to any input} \end{cases} \tag{2}$$

Given this construction, in theory one can compute y_j for any T_o as a function of R_j and τ_{ij} for all $v_i v_j$ vertex pairs. This then determines for all nodes v_i into a given node v_j which node v_i is able to 'win' and 'activate' node j if $y_j = 1$. Once the winning node 'activates' v_j it will become refractory for a period of time R_j during which $y_j = 0$, determined by its internal dynamic model. Intuitively though, note that if the state of v_j at T_o is $y_j = 0$ it could be refractory for some time $< R_j$ if had become refractory prior to T_o . This situation is interesting because we have to take into account phase shifts in the temporal properties of individual τ_{ij} and R_j at the sampling time T_o in order to understand the dynamics of the network. In fact, it is the core of much of the dynamical

richness underlying distributed signaling in a geometric network. In the next section we formalize these notions and arrive at an inequality that determines the winning vertex v_i . We then use this construction to prove a result about the bounds that define optimal efficient signaling within a network. And also show a number of practical applications of this analysis to real world networks.

Before we continue though, it is critical to note that the response of each vertex is causally independent from whatever all the other vertices in the network are doing. All that matters for computing y_j at any instantaneous time are its own internal dynamics, which determine R_j , and when signals are produced by (competing) input vertices into v_j . This is because each vertex does not have information about what all the other vertices that make up the network are doing or what their states are. It can only know its own internal state and react to the inputs it is receiving in order to decide if and when it will send out an output itself. Thus, there is a natural independence in the dynamics of the vertices that make up a network. This allows us to independently compute the interacting states of any $v_i v_j$ vertex pair at any time T_o . This is not dependent on any 'average' metric of the state or behavior of the network as a whole. In other words, it is an analytic process at a local scale that affects the dynamics of the network at the global scale. In theory, by computing *in parallel* all $v_i v_j$ state pairs one could arrive at the state of the overall network. From a practical engineering perspective, this has the advantage that the computation of the $v_i v_j$ states that make up the network can be computed using high performance computing such as graphical processing unit (GPU) architectures [6].

Finally, we note that in the explicit description we develop below we have purposely ignored any type of coupling weight between v_i and v_j , such as a synaptic weight, and focus only on the dynamic considerations that constrain the flow of signaling and information in the network. Nothing is lost by doing this; the description does not change and can accommodate a modulating weight term in y_j that represents some form of signal coupling. We show this explicitly in [6] (see equations 2.9 and 2.10 in that paper).

3.3 Signal flow dynamics between node pairs and the refraction ratio

We begin by defining a simple relationship between R_j and τ_{ij} for v_j that predicts the state y_j of v_j . It is a detailed consideration of this ratio that then provides the insights into the dynamics between v_j and the nodes that connect into it.

Definition 3.13. *The refraction ratio between the refractory period R_j for vertex v_j and the temporal signaling delay τ_{ij} into v_j for a directed connected vertex v_i on the edge e_{ij} is given by*

$$\Delta_{ij} = \frac{R_j}{\tau_{ij}} = \frac{R_j \cdot s}{d_{ij}} \quad (3)$$

where $R_j > 0$ due to corollary 3.11 and $\tau_{ij} > 0$ due to corollaries 3.9 and 3.11.

Definition 3.14. *Let $v_i(\Delta_{ij})$ be to the vertex $H_j[v_i]$ with refraction ratio Δ_{ij} for a $i = 1, 2, \dots, N$.*

Our analysis and enumeration of the combinatorial signaling space between v_i and v_j will proceed by a consideration of this ratio.

3.3.1 Unallowable conditions

There are a number of unallowable conditions that are necessitated by the physical construction of a real world network and the definitions given in section 3.1. $R = 0$ implies a non-refractory vertex capable of instantaneous recovery to an incoming signal from an upstream vertex, a condition which is not allowed (*c.f.* corollary 3.11). As $\tau_{ij} \rightarrow 0$ Δ_{ij} becomes undefined, which is equivalent to stating $d_{ij} \rightarrow 0$ since $\tau_{ij} \propto d_{ij}$ for a fixed signaling speed s , with s of course as the constant of proportionality. The theoretical limit occurs when R_j and $\tau_{ij} \rightarrow 0$. But this implies $s = \infty$ or, functionally equivalently, $d_{ij} = 0$, i.e. no geometric distances to an edge, which we discuss further below, and simultaneously infinitely fast recovery times of the internal node dynamics. But these conditions are unattainable by corollaries 3.9 and 3.11. Δ_{ij} therefore necessarily implies finite dynamic signaling and information flow in a network, as required.

3.3.2 Trivial bounds

The trivial lower bound occurs as $R_j \rightarrow 0$, $y_i = 1 \forall \tau_{ij}$. Intuitively, for any v_i into v_j when $y_i = 1$, the vertex with the shortest edge path integral will win and activate v_j . In other words, assuming a constant signaling speed s for $H_j(E)$ if we let $D_{ij} := \{d_{ij} : i = 1, 2, \dots, N\}$ be the set of all edge path integrals for $H_j(E)$, then $H_j[v_i] \rightsquigarrow v_j = v_i(\min_i d_{ij})$ for $d_{ij} \in D_{ij}$. The trivial upper bound occurs as $R_j \rightarrow \infty$, $y_j = 0 \forall \tau_{ij}$, in which case there would be no information flow or signaling in the network ever at all.

3.3.3 Refraction ratio analysis with no temporal offset

The dynamics at the network scale for any physically constructible network will depend on R_j , which in turn of course is determined by the node's internal dynamics. For any $R_j > 0$ the temporal delay τ_{ij} of a signal traveling between v_i and v_j must be such that $\tau_{ij} > 0$. The ideal will occur when τ_{ij} is as small as possible but matched to R_j ; in other words, when it is just a bit larger than R_j so that v_j responds as soon as it stops being refractory. In the informal description introduced above, if there is a number of nodes v_i with directed edges into a node v_j , the v_i that manages to achieve this condition, i.e. the signal from the upstream node v_i that reaches v_j first, will 'win' and activate v_j while immediately making it refractory to later arriving signals. We formalize these ideas in the following way. Begin by considering any two vertices v_i and v_j in a complete directed geometric graph $\mathcal{G}(V, E)$. Consider what happens when v_i signals v_j at time $t = t_i$. The shortest physically possible reaction time for v_j in all cases will be a signal reaching it from v_i just as its refractory period is ending. This occurs when $\tau_{ij} \rightarrow R_j^+$, i.e. approaches R_j from the right, that is, is slightly longer than R_j . Let Δ_{ij}^o represent the set of all Δ_{ij} ratios for all v_i vertices with directed edges e_{ij} into v_j for which the condition $\tau_{ij} \rightarrow R_j^+$ is met:

$$\Delta_{ij}^o := \{\Delta_{ij} : i = 1, 2, \dots, N, R_j/\tau_{ij} \text{ for } \tau_{ij} \rightarrow R_j^+\} \quad (4)$$

This then implies that

$$\forall \Delta_{ij} \in \Delta_{ij}^o \implies \Delta_{ij} < 1$$

We can then prove the following relation

Lemma 3.15. *Let $t_i \forall i \in \Delta_{ij}^o = t_o$, i.e. all vertices into v_j initiate a signaling event at the same time t_o . Assume v_j becomes refractory exactly at t_o . The refraction ratio Δ_{ij} for the 'winning' vertex $H_j[v_i^*] \rightsquigarrow v_j$ with $v_i^*(\Delta_{ij}^*)$ is given by*

$$\Delta_{ij}^* = \max_i \Delta_{ij} \text{ for } \Delta_{ij} > 0 \in \Delta_{ij}^o \quad (5)$$

Proof. Given the set Δ_{ij}^o , assume it is a well ordered set, i.e. there exists a smallest element in Δ_{ij}^o . Then order the elements $\Delta_{ij} \in \Delta_{ij}^o$ such that $< \Delta_{ij} \forall i = 1, 2, \dots, N$. By construction of the dynamics of the model, in the limit as $\tau_{ij} \rightarrow R_j^+$ the winning vertex $v_i^*(\Delta_{ij}^*)$ will be the vertex associated with the refraction ratio $\Delta_{Nj} = \max_i \Delta_{ij}$ as required. \square

In addition, we make the following observation about the limit of the value Δ_{ij} can take.

Lemma 3.16. *Given the set Δ_{ij}^o , $\forall \Delta_{ij} \in \Delta_{ij}^o$, if we let $\Delta_{ij,max}$ represent the largest attainable value by an element of Δ_{ij}^o ,*

$$\Delta_{ij,max} = \lim_{\tau_{ij} \rightarrow R_j^+} \frac{R_j}{\tau_{ij}} \rightarrow 1 \quad (6)$$

Proof. This follows directly from the definition of Δ_{ij} in equation 3. \square

Alternatively, we can re-write equation 5 as an inequality condition of a difference

Lemma 3.17. *Let $t_i \forall i \in \Delta_{ij}^o = t_o$. Assume v_j becomes refractory exactly at t_o . The 'winning' vertex $H_j[v_i^*] \rightsquigarrow v_j$ is given by*

$$H_j[v_{i_j}^*] = \min_i [(\tau_{ij} - R_j) > 0] \text{ for } v_i \in H_j \quad (7)$$

Proof. The necessary condition for $H_j[v_i^*] \rightsquigarrow v_j$ is $\tau_{ij} \rightarrow R_j^+$ (c.f. lemma 3.15). By lemma 3.16 in the limit $\Delta_{ij} \rightarrow \Delta_{ij,max}$ when $\tau_{ij} \rightarrow R_j$, which represents the largest value attainable by $v_{i_j}^*$. This implies that $(\tau_{ij} - R_j) \rightarrow 0$. Therefore, in every case v_i^* will be the smallest positive value of $(\tau_{ij} - R_j) \rightarrow 0$, or $\min_i [(\tau_{ij} - R_j) > 0]$ as required. Note that the condition for positive values of the difference is necessary because negative values imply that the signal from v_i arrive at v_j while it is still refractory. \square

Algorithmically, equation 7 is much more efficient to implement because one only needs to compute a difference compared to equation 5 which necessitates computing a division. This becomes significant when computing in parallel all $H_j \in G(\bar{v}, \bar{E})$.

3.3.4 Refraction ratio analysis with temporal offset

Under most conditions, there is likely to be a temporal offset between when v_i signals at t_i and how far along v_j is in its recovery from its refractory period due to a previous signaling event. This would be the case for all situations other than when v_j becomes refractory exactly at t_i as in section 3.3.3. Assume that v_i signals v_j at the same t_i for every $v_i \in H_j$, i.e. $t_i \forall i \in \Delta_{ij}^o = t_o$.

Definition 3.18. Let ϕ_j represent a temporal offset from R_j resulting in an 'effective' refractory period, such that at t_i

$$\bar{R}_j = R_j - \phi_j \text{ where } 0 \leq \phi_j \leq R_j \quad (8)$$

We re-write equation 3 as

$$\bar{\Delta}_{ij} = \frac{\bar{R}_j}{\tau_{ij}} = \frac{\bar{R}_j \cdot s}{d_{ij}} \quad (9)$$

When $\phi_j = 0$ it implies v_j became refractory exactly when v_i signaled at t_i . This is effectively the special case described by equations 5 and 7. When $\phi_j = R_j$ it implies that v_j is not refractory and can respond to an input from any v_i at any time. Note how when $\phi_j = R_j$ v_j may have been refractory at some time $t \leq t_o - R_j$, but assures the condition that $\bar{R}_j = 0$ at t_o .

Furthermore, the following lemma applies.

Lemma 3.19. Let $t_i \forall i \in \Delta_{ij}^o = t_o$. If $\phi_j = R_j$ then the edge path integral for the 'winning' vertex $H_j[v_i^*] \rightsquigarrow v_j$ with $v_i^*(\Delta_{ij}^*)$ will be $\min_i d_{ij} \forall d_{ij} \in \Delta_{ij}^o$.

Proof. Given the definition of Δ_{ij} in equation 3, for a constant s , $\Delta_{ij}^* = \lim_{\tau_{ij} \rightarrow R_j^+} \max_i \Delta_{ij}$ when $\tau_{ij} \in \Delta_{ij}^o = \min_i \tau_{ij}$ for v_i^* , since if $\phi_j = 0 \forall i \in H_j[v_{ij}]$ $y_j = 1 \forall i \in H_j[v_{ij}]$. This condition will be met when $d_{ij} \in \Delta_{ij}^o = \min_i d_{ij}$. \square

And by direct extension of lemmas 3.15, 3.16, and 3.17 we can write the equivalent expressions for $0 \leq \phi_j \leq R_j$.

Lemma 3.20. Let $t_i \forall i \in \bar{\Delta}_{ij}^o = t_o$. Assume v_j has an effective refractory period given by \bar{R}_j for some value of ϕ_j at t_o . The refraction ratio $\bar{\Delta}_{ij}$ for the 'winning' vertex $H_j[v_i^*] \rightsquigarrow v_j$ with $v_i^*(\bar{\Delta}_{ij}^*)$ is given by

$$\bar{\Delta}_{ij}^* = \max_i \bar{\Delta}_{ij} \text{ for } \bar{\Delta}_{ij} > 0 \in \bar{\Delta}_{ij}^o \quad (10)$$

Lemma 3.21. Given the set $\bar{\Delta}_{ij}^o, \forall \bar{\Delta}_{ij} \in \bar{\Delta}_{ij}^o$, and assuming v_j has an effective refractory period given by \bar{R}_j for some value of ϕ_j at t_o , if we let $\bar{\Delta}_{ij,max}$ represent the largest attainable value by an element of $\bar{\Delta}_{ij}^o$,

$$\bar{\Delta}_{ij,max} = \lim_{\tau_{ij} \rightarrow \bar{R}_j^+} \frac{\bar{R}_j}{\tau_{ij}} \rightarrow 1 \quad (11)$$

Lemma 3.22. Let $t_i \forall i \in \bar{\Delta}_{ij}^o = t_o$. Assume v_j has an effective refractory period given by \bar{R}_j for some value of ϕ_j at t_o . The 'winning' vertex $H_j[v_i^*] \rightsquigarrow v_j$ is given by

$$H_j[v_i^*] = \min_i [(\tau_{ij} - \bar{R}_j) > 0] \text{ for } v_{ij} \in H_j \quad (12)$$

In the most general case t_i for $v_i \in H_j$, i.e. the times at which each vertex initiates a signal, would not be expected to be all the same. One would expect that $t_i \neq t_o \forall i$. At any given instantaneous moment T_o a signal from any v_i may be traveling part way along e_{ij} at a speed s , effectively shortening τ_{ij} . Or it may be delayed in signaling if v_i signals some time after T_o , effectively lengthening τ_{ij} . At time T_o we need to take into account the degree of signaling progression for each edge and define $\bar{\tau}_{ij}$ analogous to \bar{R} . (Note that we write T_o to distinguish the case when $t_i \forall i \in \bar{\Delta}_{ij}^o \neq t_o$ since t_i here represents the time that vertex v_i signals, which could be different than the time T_o at which the network is observed. In effect both t_o and T_o represent an instantaneous sampling or observation time of the state of the network, but we reserve writing t_o to indicate an observation moment that coincides with all $v_i \in H_j$ signaling at the same time.)

Definition 3.23. Let τ_{ij} represent the temporal delay, i.e. latency period, for a signal to travel on the edge e_{ij} for vertex $v_i \in H_j$ when v_i initiates a signaling event at t_i and $y_j = 1$, i.e. v_j is not refractory. We then define a temporal offset for τ_{ij} , an effective shortening or lengthening of τ_{ij} as follows

$$\bar{\tau}_{ij} = \tau_{ij} + \delta_{ij} \text{ where, } \delta_{ij} \in \mathbb{R} \quad (13)$$

We extend equation 9 as

$$\Lambda_{ij} = \frac{\bar{R}_j}{\bar{\tau}_{ij}} \quad (14)$$

$\delta_{ij} > 0$ represents an effective delay or elongation beyond τ_{ij} . In other words, it represents the vertex v_i initiating a signal at some time after T_o . Values $-\tau_{ij} < \delta_{ij} < 0$ represent an effective shortening of τ_{ij} . This would be the case when v_i had initiated a signal that was traveling part way along the edge e_{ij} towards v_j prior to the sampling time T_o . When $\delta_{ij} = 0$ it implies that v_i signals exactly at the moment the network is observed. And when $\delta_{ij} = -\tau_{ij}$ it implies that the signal arrives at v_j at the moment the network is observed. Values of $\delta_{ij} < \tau_{ij}$, which result in $\bar{\tau}_{ij} < 0$, represent a signal arriving at v_j prior to the observation time T_o . We make use of this last property in section 5 below.

For completeness, we re-write equation 2 to include \bar{R}_j and $\bar{\tau}_{ij}$ as

$$\bar{y}_j(\Omega, T_o) = \begin{cases} 1, & \text{iff } v_j \text{ can respond to an input from any } v_i \\ 0, & \text{iff it is refractory to any input for a period } \bar{R}_j \text{ that begins at } T_o \end{cases} \quad (15)$$

We also similarly define

$$\Lambda_{ij}^o := \{\Lambda_{ij} : i = 1, 2, \dots, N, \bar{R}_j / \bar{\tau}_{ij} \text{ for } \bar{\tau}_{ij} \rightarrow \bar{R}_j^+\}$$

analogous to equation 4.

We first formally state the conditional relationship between $\bar{\tau}_{ij}$ and \bar{R}_j necessary for signaling.

Lemma 3.24. Let $G = (\bar{v}, \bar{E})$ represent a complete geometric graph model of a network consisting of subgraphs H_j such that all $v_i \in H_j$, i.e. $H_j(v_i)$, contain directed edges $H_j(E)$ into vertex v_j . Assume a signaling speed s_{ij} between v_i and v_j . v_i may activate v_j iff $\bar{\tau}_{ij} > \bar{R}_j$.

Proof. v_j will be in a state where it is capable of being activated in response to receiving a signal from $v_i \in H_j$ only when $\bar{y}_j(\Omega, T_o) = 1$. This is the case only following the completion of the effective refractory period \bar{R}_j . At an observation time T_o \bar{R}_j could be at any point in its temporal evolution over its range of $0 \leq \bar{R}_j \leq R_j$. In order for the signal from v_i to arrive at v_j when $\bar{y}_j(\Omega, T_o) = 1$ then, in every case $\bar{\tau}_{ij} > \bar{R}_j$. \square

And by direct extension of lemma 3.19 we can write

Lemma 3.25. *If $\phi_j = R_j$ then $\bar{R}_j = 0 \Rightarrow \Lambda_{ij} = 0$ and the 'winning' vertex $H_j[v_i^*] \rightsquigarrow v_j$ with $v_i^*(\Lambda_{ij}^*)$ will be given by the vertex with the delay $\min_i \bar{\tau}_{ij} \forall d_{ij} \in \Lambda_{ij}^o$.*

By further extending lemmas 3.20, 3.21, and 3.22 we arrive at the general theorems that completely describe the competitive refractory dynamics framework introduced in section 3.2.

Theorem 3.26. *Let $t_i \forall i \in \bar{\Lambda}_{ij}^o = \bar{\tau}_{ij}$ at T_o for some value of δ_{ij} . Assume v_j has an effective refractory period given by \bar{R}_j for some value of ϕ_j at T_o . The refraction ratio $\bar{\Lambda}_{ij}$ for the 'winning' vertex $H_j[v_i^*] \rightsquigarrow v_j$ with $v_i^*(\Lambda_{ij}^*)$ is given by*

$$\Lambda_{ij}^* = \max_i \Lambda_{ij} \text{ for } \Lambda_{ij} > 0 \in \Lambda_{ij}^o \quad (16)$$

Proof. The proof parallels the proof of lemma 3.15. Given the set Λ_{ij}^o , assume it is a well ordered set. Then order the elements $\Lambda_{ij} \in \Lambda_{ij}^o$ such that $< \Lambda_{ij} \forall i = 1, 2, \dots, N$. Due to the dynamics of the model it is still the case that in the limit as $\bar{\tau}_{ij} \rightarrow \bar{R}_j^+$ the winning vertex $v_i^*(\Lambda_{ij}^*)$ will be the vertex associated with the refraction ratio $\Lambda_{Nj} = \max_i \Delta_{ij}$ as required. In other words, in every case $H_j[v_i^*] \rightsquigarrow v_j$ will always be the vertex that arrives at v_j first subject to it recovering from its refractory period given the temporal evolution of $\bar{\tau}_{ij}$ for all i and \bar{R}_j at the instantaneous time T_o at which the network is observed. \square

Theorem 3.27. *Given the set $\Lambda_{ij}^o, \forall \Lambda_{ij} \in \Lambda_{ij}^o$, and assuming v_j has an effective refractory period given by \bar{R}_j for some value of ϕ_j at T_o , i.e. $\bar{R}_j \neq 0$, if we let $\Lambda_{ij,max}$ represent the largest attainable value by an element of Λ_{ij}^o ,*

$$\Lambda_{ij,max} = \lim_{\bar{\tau}_{ij} \rightarrow \bar{R}_j^+} \frac{\bar{R}_j}{\bar{\tau}_{ij}} \rightarrow 1 \quad (17)$$

Proof. The proof follows directly from lemma 3.16 and the definition of equations 9 and 13. \square

If $\bar{\Lambda}_{ij} = 0$ then we immediately know that v_i with $\min d_{ij} \forall v_i \in H_j(v_i)$ will win, since $\bar{\Lambda}_{ij} = 0$ only when $\bar{R}_j = 0$ which implies that $y_j(\Omega, t) = 1$.

Theorem 3.28. *Let $t_i \forall i \in \Lambda_{ij}^o = \bar{\tau}_{ij}$ at T_o for some value of δ_{ij} and c_{ij} . Assume v_j has a remaining refractory period given by \bar{R}_j for some value of ϕ_j at T_o . The 'winning' vertex $H_j[v_i^*] \rightsquigarrow v_j$ is given by*

$$H_j[v_{ij}^*] = \min_i [(\bar{\tau}_{ij} - \bar{R}_j) > 0] \text{ for } v_{ij} \in H_j \quad (18)$$

Proof. This proof parallels the proof of lemma 3.17, due again to the dependency of $v_i^*(\Lambda_{ij}^*)$ given the temporal evolution of $\bar{\tau}_{ij}$ for all i and \bar{R}_{ij} at the T_o . The necessary condition for $H_j[v_i^*] \rightsquigarrow v_j$ in this case is $\bar{\tau}_{ij} \rightarrow \bar{R}_j^+$. By theorem 3.26 in the limit $\Lambda_{ij} \rightarrow \Delta_{ij,max}$ when $\bar{\tau}_{ij} \rightarrow \bar{R}_j$, which represents the largest value attainable by v_i^* . This implies that $(\bar{\tau}_{ij} - \bar{R}_j) \rightarrow 0$. Therefore, in every case v_{ij}^* will be the smallest positive value of $(\bar{\tau}_{ij} - \bar{R}_j) \rightarrow 0$, or $\min_i[(\bar{\tau}_{ij} - \bar{R}_j)] > 0$ as required. In this case also, note that the condition for positive values of the difference is necessary because negative values imply that the signal from v_{ij} arrive at v_j while it is still refractory. \square

4 Optimized information flow

The conceptual foundation of the framework exploits the relationship between the speed of information flow in the form of signal propagation, or inversely, delay times along physical geometric edges, and the internal refractory period of individual nodes. By its construction, the framework assumes that the internal state of v_j can be computed or measured at an any time T_o and that its state $\bar{y}_j(\Omega, T_o)$ describes the refractory state for an effective refractory period of time \bar{R}_j beginning at T_o . In every case, as a function of the this effective refractory period and the effective delay time $\bar{\tau}_{ij}$ along the edge e_{ij} , the condition for the winning vertex v_i that achieves activation of v_j , i.e. $H_j[v_i^*] \rightsquigarrow v_j$, is dependent on the $\lim_{\bar{\tau}_{ij} \rightarrow \bar{R}_j^+}$. In section 2 we provided an intuitive motivating example of the effect network geometry can have on network dynamics, and informally suggested that the ability of a network to optimize its ability to efficiently maximize information flow necessitates a balance between the its geometric structure and its dynamic function. The geometry of the network is the substrate on which any dynamic function must live. Specifically, this implies a balance between how fast information is capable of propagating through the network relative to how quickly its nodes can process incoming signals. When a mismatch between network geometry and dynamics exists, it can render the network unable to process any information at all or can result in highly inefficient network dynamics. If the signaling speed s is too fast, or equivalently, if the delay times $\bar{\tau}_{ij}$ are too short compared to the amount of time a node requires to process an input and generate an output, determined by its effective refractory period \bar{R}_j , the network will not be able to sustain any internal recurrent activity. If s is too slow or the set of $\bar{\tau}_{ij}$ too long then that can render the network highly inefficient. In this section we formalize these concepts.

4.1 Optimized bounded refraction ratio

We begin by deriving upper and lower bounds on the signaling dynamics which in turn define what we mean by an optimized refraction ratio and, from that, an optimally efficient network.

Theorem 4.1 (Optimized information flow theorem). *Let $G = (\bar{v}, \bar{E})$ represent a complete geometric graph model of a network consisting of subgraphs H_j such that all $v_i \in H_j$, i.e. $H_j(v_i)$, contain directed edges $H_j(E)$ into vertex v_j . For each $v_i v_j$ vertex pair, given a signaling speed s_{ij} between v_i and v_j , assume that the state of v_j and when each v_i into v_j signaled are observed or measured at time T_o . An optimally efficient network is one where the internal dynamics are matched to the flow of signaling (information) on its edges that results in an optimized refraction*

ratio $\langle \Lambda_{ij} \rangle_{opt} \forall v_i \in G = (\bar{v}, \bar{E})$ defined by the bounds

$$\langle \Lambda_{ij} \rangle_{opt} = \lim_{\tau_{ij} \rightarrow R_j^+} \Lambda_{ij} \text{ when } \phi_j \text{ and } \delta_{ij} = 0 \quad [\text{Upper bound}] \quad (19a)$$

$$\langle \Lambda_{ij} \rangle_{opt} \Rightarrow \lim_{\delta_{ij} \rightarrow -\phi_j^+} \Lambda_{ij} \text{ when } \phi_j = R_j \quad [\text{Lower bound}] \quad (19b)$$

where τ_{ij} is the absolute signaling delay time on the edge e_{ij} and R_j is the absolute refractory period for v_j .

Proof. By lemma 3.24 the necessary condition for the activation of v_j by $v_i \in H_j$ is $\bar{\tau}_{ij} > \bar{R}_j$. By equation 8 $\bar{R}_{ij} = R_j - \phi_j$ where $0 \leq \phi_j \leq R_j$, which implies that $0 \leq \bar{R}_j \leq R_j$. \bar{R}_j is bounded by its very construction. The absolute lower bound on \bar{R}_j implies that activation of v_j by a $v_i \in H_j$ will be achieved when $\bar{\tau}_{ij} > 0$, and the absolute upper bound implies that $\bar{\tau}_{ij} > R_j$. But note how $\bar{\tau}_{ij}$ can always achieve these bounds independent of τ_{ij} for a given $v_i v_j$ pair at some observation time T_o because by equation 13 $\delta_{ij} \in \mathbb{R}$, i.e. any vertex v_i can activate v_j independent of the absolute delay time τ_{ij} by delaying the initiation of an output signal at v_i long enough if τ_{ij} is too short initiating a signal at v_i prior to T_o if it is too long. This will be true for the bounds of \bar{R}_j and any value within the range of \bar{R}_j . However, this comes at a price of inefficiency in the sense that v_i either needs to remain 'idle' for a period of time or it needs to use excess signaling resources due to having to signal prior to T_o . In both cases the requirement $\bar{\tau}_{ij} > 0$ can be met by compensating with $\delta_{ij} \ll 0$ in the case for $\bar{\tau}_{ij} \gg \tau_{ij}$ and $\delta_{ij} \gg 0$ when $\bar{\tau}_{ij} \ll \tau_{ij}$. This, in effect, intuitively implies inefficient signaling on the part of the network. However, by theorems 3.27 and 3.28, $\bar{\tau}_{ij}$ need only be slightly larger than \bar{R}_j in order to signal successfully signal v_j : $\bar{\tau}_{ij} \rightarrow \bar{R}_j^+$. But because \bar{R}_j is naturally bounded by $0 \leq \bar{R}_j \leq R_j$, it follows that the optimal signaling condition will be given by $\tau_{ij} \rightarrow \bar{R}_j^+$ for values of δ_{ij} not too smaller than zero or not too greater than zero in order to avoid compensation by δ_{ij} , which results in inefficient signaling. For the upper bound this optimized boundary condition will occur when $\tau_{ij} \rightarrow R_j^+$ when ϕ_j and $\delta_{ij} = 0$ because it represents the upper achievable limit for \bar{R}_j (when $\phi_j = 0$) and forces the optimal condition that $\tau_{ij} \rightarrow R_j^+$ without compensating with δ_{ij} . For the lower bound the optimal condition is given by $\bar{\tau}_{ij} \rightarrow 0^+ \Rightarrow \delta_{ij} \rightarrow -\phi_j^+$ when $\phi_j = R_j$, since when $\phi_j = R_j \Rightarrow \bar{R}_{ij} = 0$. Forcing the condition that $\phi_j = R_j$ implies that τ_{ij} on its own is capable of meeting the lower bound without compensation by δ_{ij} . Formally, we can define an optimized bound as $|\tau_{ij} - R_j| < \epsilon$ for some bounded error ϵ . If $\bar{\tau}_{ij}$ is too short, either because the path length of e_{ij} is too short or s_{ij} is too fast, this implies that given R_j , $\bar{\tau}_{ij} \nrightarrow R_j^+$ if $\delta_{ij} = 0$. To achieve the upper bound it would require $\delta_{ij} > 0$ so that $\bar{\tau}_{ij} > \tau_{ij}$. If $\bar{\tau}_{ij}$ is too long, either because the path length of e_{ij} is too long or s_{ij} is too slow, this implies that given R_j , $\bar{\tau}_{ij} \nrightarrow 0^+$ if $\delta_{ij} \rightarrow -\phi_j^+$. To achieve the lower bound it would require $\delta_{ij} < 0$ so that $\bar{\tau}_{ij} < \tau_{ij}$. \square

For the lower bound the important condition is that $\bar{\tau}_{ij} \rightarrow 0^+$ when $\delta_{ij} \rightarrow -\phi_j^+$. It is trivial what δ_{ij} is, since this condition will always be met when $\delta_{ij} = -\tau_{ij}$. But for the upper bound the important condition is that $\delta_{ij} \rightarrow R_j^+$ when $\delta_{ij} = 0$, which implies that in every such case $\bar{\tau}_{ij} = \tau_{ij}$.

Note that we must keep the explicit condition that $\phi_j = R_j$ because that forces $\Lambda_{ij} = 0$ only when $\delta_{ij} \rightarrow -\phi_j^+$. Otherwise, in the general case any value of $\bar{\tau}_{ij} \gg 0$ will result in $\Lambda_{ij} = 0$ for any value of \bar{R}_j .

We also have the following corollaries.

Corollary 4.2. *Given the conditions for lower and upper bounds in theorem 4.1, let $\langle \delta_{ij} \rangle_{upper}$ denote the magnitude that δ_{ij} must take in order to achieve the upper bound condition for some value of τ_{ij} that does not necessarily satisfy $\langle \Lambda_{ij} \rangle_{opt}$. Similarly, let $\langle \delta_{ij} \rangle_{lower}$ denote the absolute value that δ_{ij} must take in order to achieve the lower bound condition for some value of τ_{ij} that does not necessarily satisfy $\langle \Lambda_{ij} \rangle_{opt}$. In every case, the relationship between $\langle \delta_{ij} \rangle_{upper}$ and $\langle \delta_{ij} \rangle_{lower}$ is given by*

$$\langle \delta_{ij} \rangle_{lower} = \langle \delta_{ij} \rangle_{upper} - R_j$$

Proof. The condition for the upper bound is $\tau_{ij} \rightarrow R_j^+$ for $\delta_{ij} = 0$ (and $\phi_j = 0$). With a bit of abuse of the relational terms, since $\bar{\tau}_{ij} = \tau_{ij} + \delta_{ij}$, under these conditions if $\tau_{ij} \neq R_j$ then $\bar{\tau}_{ij} \rightarrow R_j^+$. For a given τ_{ij} and for a known or measurable R_j , $\langle \delta_{ij} \rangle_{upper} = -(\tau_{ij} - R_j)$, since this is what the value of δ_{ij} would have to be in order to achieve the optimal condition. For the lower bound $\bar{\tau}_{ij} \rightarrow 0^+$ when $\delta_{ij} = -\phi_j$ given that $\phi_j = R_j$. Thus, if $\tau_{ij} - \phi_j \equiv \tau_{ij} - R_j > 0$, or more correctly if $\bar{\tau}_{ij} \rightarrow 0^+$, it implies that $\langle \delta_{ij} \rangle_{lower} = -\tau_{ij}$ would be needed to meet the lower bound optimality condition. The difference between $\langle \delta_{ij} \rangle_{lower}$ and $\langle \delta_{ij} \rangle_{upper}$ is therefore $-\tau_{ij} - [-(\tau_{ij} - R_j)] = -R_j$. Thus, $\langle \delta_{ij} \rangle_{lower} = \langle \delta_{ij} \rangle_{upper} - R_j$. \square

Corollary 4.3. *If a signal $v_i \in H_j(v_i)$ characterized by a delay time τ_{ij} on the edge e_{ij} is able to achieve either the optimal upper bound or optimal lower bound as defined in theorem 4.1, then it is guaranteed to be able to achieve the other optimal bound.*

Proof. Asking if a signal capable of achieving the upper bound can also achieve the lower bound is equivalent to asking if $\bar{\tau}_{ij} \rightarrow 0^+$ when $\tau_{ij} = R_j$. But the condition for the lower bound is $\bar{\tau}_{ij} \rightarrow 0^+$ when $\delta_{ij} = -\phi_j$. Substituting for these explicit variables we arrive at

$$\begin{aligned} \bar{\tau}_{ij} &= \tau_{ij} + \delta_{ij} \\ &= R_j - \phi_j \end{aligned}$$

but since $\phi_j = R_j$ for the lower bound, it implies that $\bar{\tau}_{ij} = 0$, or more appropriately, $\bar{\tau}_{ij} \rightarrow 0^+$.

Asking if a signal that satisfies the optimality condition for the lower bound can also achieve the upper bound is equivalent to asking if $\bar{\tau}_{ij} \rightarrow R_j^+$ when $\delta_{ij} \rightarrow -\phi_j$. Similarly,

$$\begin{aligned} \bar{\tau}_{ij} &= \tau_{ij} + \delta_{ij} \\ 0 &= \tau_{ij} - R_j \\ \tau_{ij} &= R_j \end{aligned}$$

which implies that the optimality condition for upper bound is satisfied. \square

4.2 Optimally efficient networks

We can then define an optimally efficient network in the following straightforward way:

Definition 4.4. (*Optimally efficient network*) In every case, as a function of the effective refractory period and effective delay time $\bar{\tau}_{ij}$ along the edge e_{ij} , the condition for the winning vertex v_i that achieves activation of v_j , i.e. $H_j[v_i^*] \rightsquigarrow v_j$, is dependent on the $\lim_{\bar{\tau}_{ij} \rightarrow \bar{R}_j^+} \forall v_i \in G(V, E)$. When this condition is satisfied for all edges $H_j(E)$ for all sub-graphs $H_j \in G$ in the network the network is optimally efficient, i.e. $\langle \Lambda_{ij} \rangle_{opt} \forall v_i \in G(V, E)$

5 Optimal efficiency in real world natural and engineered networks

An optimally efficient network is one where the internal dynamics are matched to the flow of signaling (information) on its edges as given in theorem 4.1 and definition 4.4. Any network with v_i, v_j node pairs for which $\Lambda_{ij} \neq \langle \Lambda_{ij} \rangle_{opt}$ will progressively deviate from optimal efficiency in its ability to dynamically represent and process information. A natural question to ask then is if real world networks, either naturally occurring networks or engineered networks, have evolved or have been designed, respectively, so that they approach optimally efficient networks. While we leave a detailed analysis of specific real world networks to future work, we briefly propose empirical evidence that suggests that real world networks can be optimally efficient, across three completely distinct topics and application areas.

5.1 Biological neuronal networks

We first considered synaptic signaling in biological neural networks. Spiking biological neurons that produce action potentials have an absolute refractory period extending out to about 0.8-1 ms. The absolute refractory period is mediated by the inactivation of populations of sodium channels responsible for the depolarizing phase of the action potential. During this period other incoming stimuli cannot elicit another response from that neuron. In neurons the integrative combinatorial nature of the interactions from presynaptic neurons synapsing on a post-synaptic neuron is exceedingly complex due to synaptic dendritic integration prior to reaching the threshold potential at the initial segment that triggers an action potential; much more so than the first order approximation we conceptually built into our theory. Neurons also have a relative refractory period that typically lasts to about 5 ms due to the potassium mediated after hyperpolarization and recovery times of the sodium channels that result in necessitating larger than typical stimuli in order to have a chance to produce subsequent action potentials. Furthermore, typical chemical synapses have synaptic delays on the order of 1-5 ms, and longer in some cases. We do not elaborate further on the details of the neurophysiology here but direct the interested reader to the standard texts in the field. In the context of the theory we develop here, collectively the biological absolute and relative refractory period represent the framework's absolute refractory period of neurons, R_j . Axonal conduction delays, the period of time it takes for action potentials to propagate down the length of the axon, represents the delay time τ_{ij} between the presynaptic neuron through which the action potential is propagating (node v_i) and the postsynaptic neuron it is passing along the signal to (node v_j). Conduction delays are a function of the action potential (signaling) propagation speed down the axon, which is itself a function of several variables including axon diameter and axonal myelination, and the length of

the axon itself. Axon lengths can vary significantly depending on whether they are long range or local connections for example. As such, there is a tremendous degree of variability in axonal conduction delays across different neuronal populations, brain regions, and across species. (See Table 1 in http://www.scholarpedia.org/article/Axonal_conduction_delays for example). Yet, in every case for all neurons seems to be a regime a regime that can be found in the conduction delays such that the effective temporal delays (equation 13, $\bar{\tau}_{ij} = \tau_{ij} + \delta_{ij}$ where, $\delta_{ij} \in \mathbb{R}$) matches the effective refractory period (equation 9, $\bar{R}_{ij} = R_j - \phi_j$ where $0 \leq \phi_j \leq R_j$), resulting in an optimized refraction ratio $\langle \Lambda_{ij} \rangle_{opt}$.

Budd and colleagues recently investigated in detail the relationship between the amount of material a neuron commits to its axonal arbor, the branching points where the axon synapses with various postsynaptic neurons, and conduction delay times [5]. Originally proposed by Santiago Ramon y Cajal and subsequently adopted by many groups, the prevailing dogma was that a neuron optimizes resources in order to minimize the amount of cellular material it uses in its axonal arborization. However, as Budd and colleagues showed this comes at the price of increased conduction delays. These authors showed that a neuron sacrifices material in order to achieve shorter conduction delays, representing a trade off between anatomical optimization and dynamics. They first carried out detailed tract tracing of excitatory spiny and pyramidal cells and inhibitory large basket cell in the in vivo cat neocortex, and then compared axonal path lengths and conduction delays (given knowledge of the range of conduction speeds in these neurons) with graph theoretic models optimized for shortest physical paths (i.e. conservation of material) or paths that provided the most efficient conduction times. Their results suggest that neurons are neither optimized for conservation of cellular material nor for the shortest conduction delays possible, but instead fall in a regime in between these two extremes. They also showed that there is a scaling effect where this balance is maintained independent of the number of synaptic boutons (terminals) a neuron branchings into. The authors go on to suggest that the design of intracortical arbors are tailored to support a high degree of temporal precision in the timing of when action potential occur, which underlies how they contribute to neuronal signaling (so called temporal dispersion- which is critical to rate code models of neuronal signaling, see for example [9, 17, 19]). And that neurons closely preserve and regulate the relationship between distance and latency.

What this paper does not strictly address is why such a trade off exists in the first place. Interpreting their results in the context of our theory suggests a possible answer to this question. The results of Budd et. al. imply that neurons put significant resources in the form of cellular material into maintaining a constant conduction delay for all synapses, independent of the specifics of the axonal arborization. In other words, all other things being equal two neurons synapsing onto the same post synaptic neuron would have equal opportunity for contributing to the generation of an action potential as a result of dendritic integration at any instantaneous moment in time, omitting of course other important considerations such as synaptic coupling strength and ‘by design’ differences in how different classes of neurons synapse on a postsynaptic dendritic arbor, e.g. clustering of inhibitory synapses closer to the soma. This makes sense etiologically because the establishment of synaptic connections is not deterministic but stochastic, in the sense that while there is a high level pre-programmed plan for how a developing brain should be wired up, individual synaptic connections between specific neurons are not hard coded. If this was not the case then stochastic connectivity effects at the level of cellular neural circuits and networks could have a disproportionate degree of influence on neural signaling and information processing at the network scale, which would

ultimately affect the ability of the brain to function properly. Given the definition of $\langle \Lambda_{ij} \rangle_{opt}$ and theorem 4.1, at a constant signaling speed, a lack of distance (path length) preservation in axonal arbors would stochastically make specific pre- postsynaptic neuronal node pairs more or less efficient. Information in the brain at the level of individual neurons and neural circuits is tightly tied to the timing effects of action potentials. So in order for neurons to be on equal footing with regards to temporal dispersion, conduction delays must be tightly regulated and preserved. This is what our theory predicts and what Budd et. al. have independently demonstrated experimentally. Our theoretical interpretation suggests the reason why neurons and neuronal networks are designed the way they are.

We further explored this in simulations. It is surprisingly difficult to get specific and accurate data on axonal and axonal arbor cellular anatomical path lengths along with simultaneous conduction velocities. To a first approximation we used data provided in [5], who carried out detailed anatomical tract tracing reconstructions of sample spiny cortical neurons and basket cells in adult cat primary visual cortex (see for example their Figs. 4, 5, and 12). Spiny cell axonal arbors, which we considered in our simulations, range from just over zero to just under 4 mm in length (median = 1.66 mm with a standard deviation of 0.77 mm). In our simulations we used a path length range of 1 to 3.8 mm. Axonal conduction velocity is a function of axonal diameter, branching, ion channel sub-types and density, and myelination [5, 7], although numerical simulations suggest that path length is the most significant determinant of conduction velocity [14]. Reported values of neuronal conduction velocities in adult cat visual cortex differ rather significantly depending on the study. We used a range of 0.1 to 0.6 m/sec, which is a range that covers most of the reported values [4, 12, 13]. Using this as a starting point, we first computed conduction signaling delays τ_{ij} as a function of the path length and conduction velocity ranges (Fig. 3a.). This yielded a maximum conduction delay of just under 40 ms. We then computed the the refraction ratio Λ_{ij} as a function of τ_{ij} and the refractory period R_j . There is very little direct data on the refractory periods of spiny neurons that we are aware of, and as such we assumed a refractory period range of 0.8 to 5 ms, as described above. Within these computed ranges, the surface of Λ_{ij} extends from a maximum value of 3 to a minimum of 0.021. There exists a subset of Λ_{ij} that displays near optimal efficiency, indicating that within the experimental limitations of the available measured data to date, spiny neurons are capable of achieving dynamic optimally efficient signaling that approaches $\langle \Lambda_{ij} \rangle_{opt}$ for a range of appropriate combinations of the key contributing parameters, namely, path length, conduction velocity, and refractory period. We considered parameter ranges that resulted in refraction ratios bounded by $0.8 \leq \Lambda_{ij} \leq 1.2$ as near optimal, i.e. approaching $\langle \Lambda_{ij} \rangle_{opt}$. The smallest value of R_j that resulted in a ratio of $\Lambda_{ij} = 0.8$ occurred at 1.34 ms, with $\tau_{ij} = 1.6667$ ms. The smallest value of τ_{ij} that resulted in a ratio of $0.8 = 5$ ms, with $R_j = 4ms$. Smallest value of R_j that produce a ratio of 1.2 occurred at 2 ms, with $\tau_{ij} = 1.6667$ ms; while the smallest value of τ_{ij} that resulted in a ratio of 1.2 was at 3.333 ms, with $R_j = 4$ ms. It should be noted however, that this analysis was performed at the level of individual neuron-neuron node-node pairs, and not at the scale of the entire network (*c.f.* definition 4.4).

5.2 Internet packet processing and routing

We also briefly considered internet routing where the theory suggests a scenario that is contrary to a 'standard' analysis of the problem. Ramaswamy et. al. provide a good concise introduction to

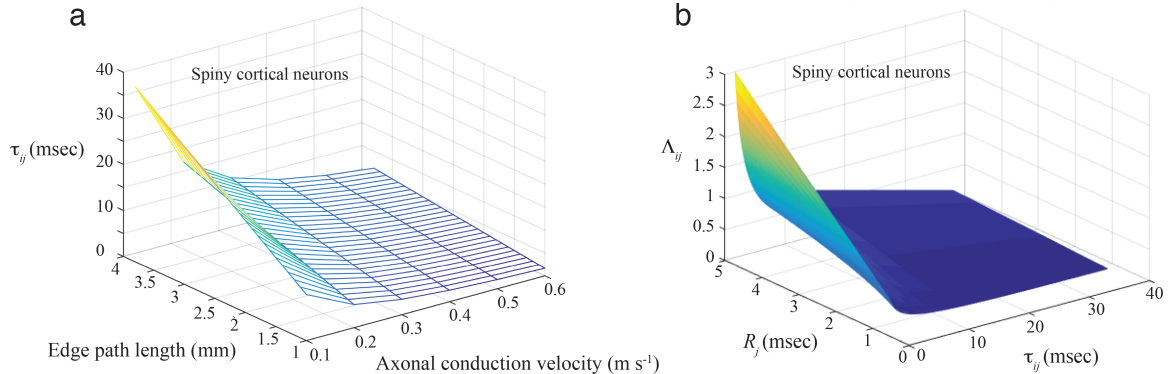


Figure 3: Computed conduction (signaling) delays τ_{ij} and refraction ratios Λ_{ij} (panel b.) for spiny cortical neurons in the adult cat primary visual cortex. The two dimensional surface of τ_{ij} was computed from experimentally measured ranges of path length and axonal conduction velocities derived from the published literature (**panel a.**), while Λ_{ij} (**panel b.**) was computed from the data in panel a. along with refractory period estimates of mammalian central neurons.

the current demands placed on packet routing on the internet [16]. Borrowing from these authors' own description: The internet has evolved from its original functionality as a store and forward network to a much more complex and sophisticated communication infrastructure. The needs required by network security and performance necessitates network traffic that is processed within the network in addition to packet forwarding and routing. This processing occurs primarily on routers as opposed to end systems, and include critical processes and applications such as network address translation (NAT), firewalling, and virtual private network (VPN) tunneling. These authors then go on to make the point that other complex services place even greater demands on packet processing at the router level, including virus scanning, content adaptation for wireless clients, and ad insertion in web page requests. In their paper they investigated the (increasing) temporal delays associated with increasing router level processing of packets. Sending a packet from one node in the network to another can experience delays associated with transmission delays, the time it takes to transmit a packet, propagation delays, the time it takes to actually transmit a packet, the processing delay, which is the time it takes to handle the packet on the network, and queuing delays, the amount of time the packet is buffered before it can be sent. In the context of our theory the combination of transmission and propagation delays collectively contribute to the representation of τ_{ij} . The processing and queuing delays map to R_j . Table 1 provides measured delay times for the different classes of delays associated with packet routing (*c.f.* table 1 in [16]), along with the computed refraction ratio Λ_{ij} for each set of data. The computed values of Λ_{ij} in the table intentionally ignore queuing delays, since these can range from zero to infinite, depending on the amount of buffering taking place. But we will come back to this consideration. While τ_{ij} , the time it takes to actually transport a packet through the network, does not change as the packet goes from a simple to a more complex payload, R_j increases by two orders of magnitude. The increased demands on the processing time associated with complex packet manipulations necessary to meet the needs of ever increasing advanced and sophisticated applications that depend on such

Type of delay	Simple packet forwarding (μs)	Complex payload modifications (μs)	Contribution to the refraction ratio Λ_{ij}
Transmission delay	10	10	τ_{ij}
Propagation delay	1000	1000	τ_{ij}
Processing delay	10	1000	R_j
Queuing delay	10 to infinity	10 to infinity	R_j
Refraction ratio Λ_{ij}	0.0099	0.99	

Table 1: Internet router network delay times and computed refraction ratios. Transmission and propagation delays contribute to τ_{ij} , while processing and queuing delays contribute to R_j . Note that the computed values of Λ_{ij} in the table intentionally ignore queuing delays. See text for details. Data adapted from Table 1 in [16].

increased functionality is understandably a consideration and even concern for the efficient design of the internet infrastructure. However, comparing the refraction ratios for simple versus complex packets suggest that simple packet routing is inefficient and far from optimal because of a mismatch between the transmission and propagation times versus the processing time ($\Lambda_{ij} = 0.0099$, assuming all routers and the links between them display the same dynamics), the former being much slower than the amount of time a simple packet is handled by a router itself. While the processing time of a complex packet increases significantly by two orders of magnitude, at current estimates the increase in the amount of time a router needs to hold onto a packet to carry out these additional operations is such that it almost perfectly matches the temporal delay associated with the propagation of packets through the network, which brings the refraction ratio to optimal ($\Lambda_{ij} = 0.99$). From a network design and resource allocation and management perspective, this simple analysis suggests that no changes to the network need occur for existing complex packets. However, it does point to a saturation of the temporal resources available to the router as the demands on it continue to increase given existing protocols and algorithms. Any future increases in processing times will cause a deviation from dynamic optimality, but this time with $\Lambda_{ij} > 1$ due to increasing R_j . These are considerations that could play an important role in design and resource allocation considerations for future iterations of the internet. Finally, we note how the theory we develop here can provide a guide for network design and dynamic analysis, but ultimately domain specific considerations must determine how the refraction ratio is computed. In the example here we chose to ignore queuing delays due to their significant variability. Clearly though, the inclusion of such a delay will impact the value of Λ_{ij} , but deciding how such a variable is included, when, and the weight it carries is dependent on the specifics of the network and system under consideration. However, an analysis similar to the simple example we discuss here could provide a powerful tool for testing the relative contributions of different variables to the dynamic efficiency of a network, in support of informed and systematic network design decisions.

5.3 Prevalence of small world networks

In 1998 Watts and Strogatz published their seminal paper introducing small world networks, and suggested that this topology could be pervasive across both nature and engineered networks [20]. The small world network connectivity structure lives between a completely random network and a regular lattice. It provides an opportunity for nodes that would normally not be connected to be connected, resulting in a 'short circuiting' of dynamical behaviors and communication between different parts of the network that would normally not be in such immediate and direct contact. In essence, signals have the opportunity to spread faster and reach farther due to the presence of sparse long range connections in an otherwise locally connected network. A key observation of this work was that the transition to a small world topology from a regular lattice is essentially undetectable at the local scale, but can have significant effects on the dynamics and the spread of information. What is less obvious though, is *why* this network topology should be so prevalent. Our theory suggests an intriguing explanation. First, consider a random network, where there is a uniform probability of any two nodes being connected regardless of their positions in the network. Random networks, despite their long history of study within graph theory, cannot be optimal efficient networks as we define them here, assuming similar internal node dynamics and a uniform signaling speed. To see why, consider that if $\Lambda_{ij} = \langle \Lambda_{ij} \rangle_{opt}$ for a particular or specific $v_i \in G(V, E)$, it implies that $\Lambda_{ij} = \langle \Lambda_{ij} \rangle_{opt} \forall v_i \in G(V, E)$. But this condition cannot be met for a random network because there would be a distribution of edge path lengths but only a small subset would produce signaling delays or latencies that match whatever are the internal dynamics of the nodes in the network. Now consider the small world topology in the following way. Define a cost function associated with deviation of an optimal refraction ratio for a $v_i v_j$ node pair, given that to achieve the optimal bounds in every case $\tau_{ij} \rightarrow R_j^+$. This condition is met when $-\phi_j \leq \delta_{ij} \leq 0$ (theorem 4.1). We can define a cost function as $C_{ij} = |\tau_{ij} - R_j|$ for every connected vertex pair and then average over the entire network:

$$C_N = \frac{\sum_{k=1}^K C_k}{K} \text{ for } k = 1, 2, 3 \dots, K \text{ edges} \quad (20)$$

For edges with $\tau_{ij} > R_j$ the cost function can distinguish long edges since for short edges $0 < C_{ij} < R_j$. However, for simplicity it does not distinguish between signaling delays for $R_j < \tau_{ij} \leq 2R_j$, which results in the same cost. Presumably, edges that are excessively long will require excess physical resources to be constructed, so it makes sense that the cost be greater, similar to the basis of the arguments associated with axonal branching material conservations laws in neurons. However, it is more difficult to say what the real cost should be for a limited amount of excess material (for long edges when $R_j < \tau_{ij} \leq 2R_j$) versus a shorter edge that may require a wait before signaling.

A regular lattice network with probability p of long range random re-wirings equal to zero (see [20] for details), can be made to exhibit arbitrarily near optimal signaling dynamics approaching $\langle \Lambda_{ij} \rangle_{opt}$ since the speed of signal propagation can balance the length of the edges such that they match the internal node dynamics. Because it is a regular lattice network, with all edges being equal, such an appropriate signaling delay will apply to the entire network and $C_N \rightarrow 0$. As these authors pointed out, the impact of the small world topology comes from the fact that even a few long range randomly re-wired edges have a significant effect on information flow and network dynamics while essentially having no effect at the local node scale of a lattice network. As they point out, "... at the local level ... the transition to a small world is almost undetectable". Given our theoretical development

here, we can now understand why this is the case: assuming consistent internal node dynamics and a constant signaling speed on all edges, sparse long range random re-wiring events in a small world network sufficient to produce a meaningful effect on network dynamics can be constructed from an optimally efficient regular lattice network with essentially no effect on a loss of optimization. We further explored this concept empirically. The clustering coefficient in a small world network, $C(p)$, is a measure of the degree of local connectivity. It reflects the deviation of a small world network from a regular lattice network at the local scale. (See Fig. 2 in [20] for a formal definition.) $C(p)$ is nearly constant and unchanging from a lattice network until about $p = 0.01$ ($C(p)/C(0) = 1$, where $C(0)$ represents a value of $p = 0$ which denotes no random rewiring and a lattice network structure.) In contrast, the characteristic path length $L(p)$ for $p = 0.01$ as a ratio of the characteristic path length of a lattice network $L(0)$ is $L(p)/L(0) \simeq 0.2$, indicating a significant degree of long range re-wiring events at the scale of the whole network. $L(p)$ is a measure of the shortest path between two vertices, averaged over the entire network. If we then consider the network optimization cost C_N as a function of p we observe that at the critical transition probability $p = 0.01$ there is essentially a negligible change in C_N relative to a optimized regular lattice network (Fig. 4). We considered C_N for families of small world networks with increasing random re-wirings starting from a regular lattice network that had a refraction ratio $\Lambda_{ij} = 1.2 := \langle \Lambda_{ij} \rangle_{opt} \forall v_i \in G(V, E)$ for all vertex pairs. We then investigated how C_N changed as a function of increasing p for small world networks where the random re-wirings produced longer edges that were $2x$, $10x$, and $20x > \langle \Lambda_{ij} \rangle_{opt}$ for re-wired vertex pairs. In all cases, $\Delta C_N < 0.019$ at $p = 0.01$ even though $\Lambda_{ij} = 1.667$ (for the curve labeled $2x$), 8.333 (curve labeled $10x$), and 16.667 (curve labeled $20x$). In other words, even though the signaling efficiency for each of the three networks (by design) progressively deviated from $\langle \Lambda_{ij} \rangle_{opt}$, the additional deviation from $\langle \Lambda_{ij} \rangle_{opt}$ introduced by random re-wirings associated with a small world network, measured by the cost function C_N was essentially negligible at re-wiring probabilities that produce significant effects on network dynamics attributed to the small world topology. Specifically, at a re-wiring probability $p = 0.01$. We then explored how C_N changes at fixed p values as a function of increasing re-wiring signaling delays, expressed again as x times greater than the signaling speed associated with $\langle \Lambda_{ij} \rangle_{opt}$ (Fig. 5). The change in C_N was linear but with different slopes, reflecting the value of p . While there is an increase in C_N associated with re-wired edges that have signaling speeds that progressively move Λ_{ij} away from $\langle \Lambda_{ij} \rangle_{opt}$, as would be expected, the change is linear and rather flat. Lastly, we explored how C_N changed as a function of p for different deviations from $\langle \Lambda_{ij} \rangle_{opt}$ for the starting regular lattice network (Fig. 6). Increasing the initial deviation from $\langle \Lambda_{ij} \rangle_{opt}$ for all vertex pairs in the starting lattice network did not change the dynamics of how C_N varied, but did affect the starting value of C_N across all values of p .

Taking into consideration our theoretical considerations, small world networks represent a connectivity class which can be designed to display arbitrarily optimal signaling dynamics with essentially negligible deviation from regular lattice networks while simultaneously displaying sufficient long range random edge re-wirings (e.g. at $p = 0.01$) to produce a significant impact on the dynamics of the network. It makes sense for both natural and engineered networks to take advantage of this topological structure, since it provides a simple set of construction rules to produce tailored effects on dynamics and the propagation of information through the network (via the re-wiring probability p) with essentially no resource costs in doing so.

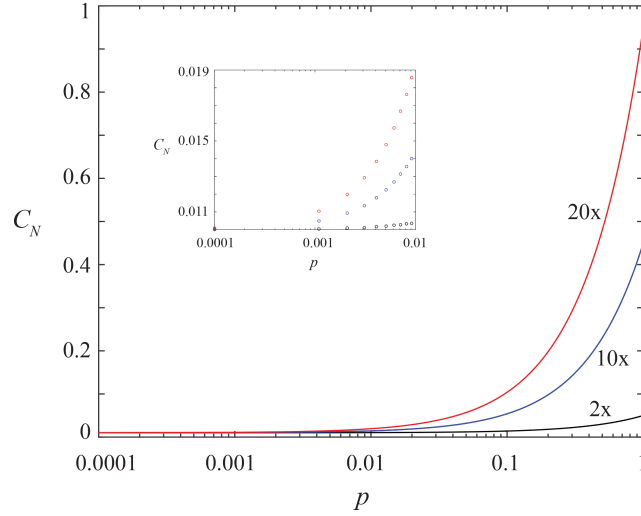


Figure 4: Network cost function C_N as a function of small world re-wiring probability p for three networks with differing deviations of dynamic signaling optimality for re-wired edges. The starting lattice network was considered optimally efficient with $\Lambda_{ij} = 1.2 := \langle \Lambda_{ij} \rangle_{opt}$. Randomly re-wired long range connections had signaling delays of 2x, 10x, and 20x $> \langle \Lambda_{ij} \rangle_{opt}$. Inset: Magnified C_N scale up to $p = 0.01$.

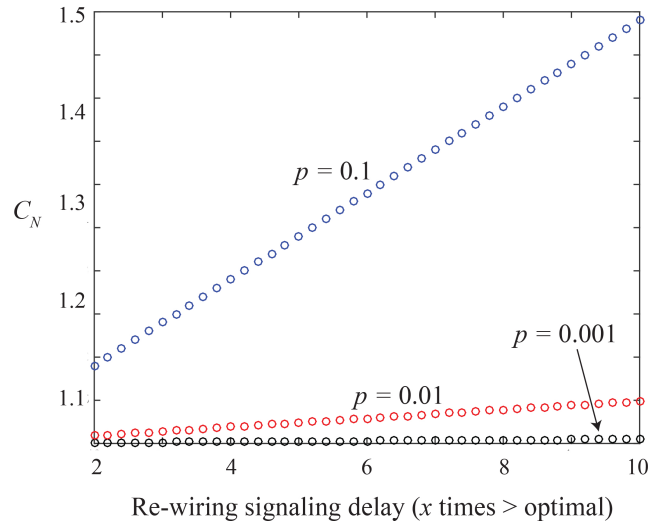


Figure 5: Network cost function C_N as a function of increasing re-wiring deviation from $\langle \Lambda_{ij} \rangle_{opt}$ for small world network. C_N was computed for value of $p = 0.001, 0.01,$ and 0.1 .

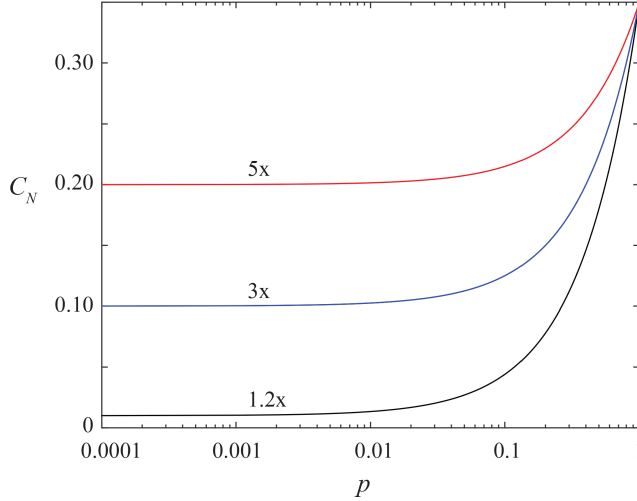


Figure 6: Network cost function C_N as a function of small world re-wiring probability p for three networks with differing deviations from $\langle \Lambda_{ij} \rangle_{opt}$ for the starting lattice network. Signaling delays for the starting lattice network were 1.2, 3x and 5x $>$ than $\langle \Lambda_{ij} \rangle_{opt}$.

6 Discussion

In this paper we have described an intuitively and conceptually simple framework that describes the dynamics of signaling and information flows in complete geometric networks. An important result is the derivation of the bounds that define the optimized refraction ratio, $\langle \Lambda_{ij} \rangle_{opt}$ via the optimized information flow theorem (theorem 4.1). This theorem provides a quantitative foundation for what it means for a network to be dynamically optimally efficient in how signals (information) propagates through its edges. We propose that such an analysis can be carried out for any physically realizable real world network to provide insights into their behaviors and dynamics, or to guide their design, since the dynamics can be predicted by the theory. In this paper we briefly explored this in the context of biological neural networks, the internet routing network, and the small world topology. Some theoretical aspects of the framework were intentionally left open in order to provide sufficient application specific flexibility in how the theory can be used. For example, the situation where there is a tie with regards to two signals reaching a node v_j at exactly the same moment. We did not attempt to explicitly account for this because the details of how such a tie is broken is a property of the specifics of the system itself. Consider as an example Watt's and Strogatz's simulation of the spread of infections as a function of the small world topology (see their Fig. 3 in [20] and its accompanying text). The tie breaking rule in this case is that if two vertices are at the same time step attempting to infect the same v_j there is no competition at all and no tie breaking rule is needed. Either v_j will be infected given the respective probabilities of each v_i (or the same probability for a given r_i equal for the whole network) or it will not. The competitive refractory dynamics in this model only exists at the level of nodes attempting to reach uninfected nodes at a given time step.

Finally, in many ways the work we introduce here is just a beginning. Future theoretical work will address a more general version of the framework capable of accommodating heterogeneity in the network, such as variable s_{ij} across different $v_i v_j$ node pairs or even on different parts of the same edge, and varying classes of nodes within the same network that result in differing R_j values. We anticipate that this will lead to very interesting signaling and information flow dynamics on the network. Such a generalized theory will be applicable to many types of real world networks, such as for example signaling across different networks of distinct populations of neurons in the brain. Other theoretical work will explore possible links that map the concepts and formal descriptions in our theory to other distinct theoretical work. These may include connections to Markov processes and the growing literature of adaptive networks. There may be deep theoretical associations we are not yet aware of. Finally, there may be opportunities to explore new theoretical terrains. For example, the development of the competitive dynamics framework and optimized information flow bounds in non-Euclidean geometric networks. Asking this of course implies a certain amount of development and foundational knowledge of geometric networks in one of the other non-Euclidean geometries. While a fascinating topic to consider, to the best of our knowledge such a development is very limited. In terms of practical applications of the theory we believe that use of the framework for the analysis of both natural and engineered networks in order to learn about the foundational mechanisms underlying their dynamics will be an important and productive direction. Conversely, as we have already emphasized, there is significant opportunities for using the theory to systematically design networks with specific dynamics and behaviors, and to test the performance and operational limits of networks with a given structure.

Acknowledgments

I am very grateful to Prof. Fang Chung (Department of Mathematics, UC San Diego), Prof. Shankar Subramaniam (Department of Bioengineering, UC San Diego), and Dr. Marius Buibas, for their input and many hours of fruitful discussions. This work was supported by grants 63795EGII and N00014-15-1-2779 from the Army Research Office (ARO), United States Department of Defense.

References

- [1] R Albert and A L Barabási. Statistical mechanics of complex networks. *Reviews of modern physics*, 74:47–97, 2002.
- [2] D Archdeacon. Topological graph theory: a survey. *Congressus numerantium*, 115:5–54, 1996.
- [3] C P Bonnington and C H C Littele. *The foundations of topological graph theory*. Springer, 1995.
- [4] V Bringuier, F Chavane, L Glaeser, and Y Frégnac. Horizontal propagation of visual activity in the synaptic integration field of area 17 neurons. *Science*, 283:695–699, 1999.

- [5] Julian M L Budd, Krisztina Kovács, Alex S Ferecskó, Péter Buzás, Ulf T Eysel, and Zoltán F Kisvárday. Neocortical axon arbors trade-off material and conduction delay conservation. *PLoS Comput Biol*, 6:e1000711, 2010.
- [6] Marius Buibas and Gabriel A Silva. A framework for simulating and estimating the state and functional topology of complex dynamic geometric networks. *Neural Comput*, 23:183–214, 2011.
- [7] D Debanne. Information processing in the axon. *Nature Reviews Neuroscience*, 5:304–316, 2004.
- [8] S N Dorogovtsev, A V Goltsev, and JFF Mendes. Critical phenomena in complex networks. *Reviews of Modern Physics*, 80:1275–1335, 2008.
- [9] P Fries, S Neuenschwander, A K Engel, and R Goebel. Rapid feature selective neuronal synchronization through correlated latency shifting. *Nature*, 4:194–200, 2001.
- [10] T Gross and B Blasius. Adaptive coevolutionary networks: a review. *Journal of The Royal Society, Interfaces*, 5:259–271, 2008.
- [11] T Gross and H Sayama. *Adaptive Networks*. Springer Science, 2009.
- [12] J A Hirsch and C D Gilbert. Synaptic physiology of horizontal connections in the cat’s visual cortex. *The Journal of Neuroscience*, 11:1800–1809, 1991.
- [13] H J Luhmann and J M Greuel. Horizontal Interactions in Cat Striate Cortex: II. A Current SourceDensity Analysis. *European Journal of . . .*, 2:358–368, 1990.
- [14] Y Manor, C Koch, and I Segev. Effect of geometrical irregularities on propagation delay in axonal trees. *Biophysical Journal*, 60:1424–1437, 1991.
- [15] H Pach. *Thirty essays on geometric graph theory*. Springer, 2013.
- [16] R Ramaswamy, N Weng, and T Wolf. Communications processing delay. *IEEE Global Telecommunications Conference, 2004*, 3:1629–1634, 2004.
- [17] M Rudolph and A Destexhe. Tuning neocortical pyramidal neurons between integrators and coincidence detectors. *Journal of computational neuroscience*, 14:239–251, 2003.
- [18] H Sayama, I Pestov, J Schmidt, and B J Bush. Modeling complex systems with adaptive networks. *Computers and mathematics with applications*, 65:1645–1664, 2013.
- [19] W Singer. Neuronal synchrony: a versatile code for the definition of relations? *Neuron*, 24:49–65, 1999.
- [20] D J Watts and S H Strogatz. Collective dynamics of ‘small-world’ networks. *Nature*, 393:440–442, 1998.